

# Stationary and switching synchronization regimes in an ensemble of four nonidentical phase oscillators with repulsive couplings

A.V. Bobrova<sup>a)</sup> and G.V. Osipov

(\*Electronic mail: alla.bobrova@unn.ru)

(Dated: 21 November 2025)

This study investigates the collective dynamics (phase synchronization, instantaneous frequencies synchronization and mean frequencies synchronization) in an ensemble of four nonidentical phase oscillators with repulsive coupling. We use the Kuramoto-Sakaguchi system of ordinary differential equations as our mathematical model. Depending on the coupling strength in the presence of a small mismatch of the natural frequencies, all possible modes of frequency synchronization were found: 4:0 (global), 3:1, 2:2, 2:1:1 (cluster). It is shown that these regimes can be classified into two main types depending on the evolution of the instantaneous frequencies: stationary (4:0 and 2:2), characterized by constancy of phase ratios and instantaneous frequencies, and switching (3:1 and 2:1:1), in which metastable processes with periodic switching of synchronous states are observed: for different time intervals, different types of locking of instantaneous frequencies of oscillator pairs and different types of phase ratios were observed. For the 4:0 and 2:2 regimes, analytical expressions for the synchronization frequencies were derived. The presence of bistability has been revealed depending on the initial conditions of different synchronous regimes at the same parameters: sets of individual frequencies and value of coupling strength.

**The collective dynamics of coupled phase oscillator ensembles exhibits a wide range of phenomena, including global and partial (clustered) synchronization. Although partial synchronization in such ensembles is a well-known phenomenon, the underlying mechanisms and the classification of regimes in systems with *nonidentical* elements and *repulsive* coupling require further investigation. In this paper we study a system of four phase oscillators and demonstrate that repulsive coupling combined with a small frequency mismatch leads not only to conventional stationary regimes (global 4:0 synchronization and pairwise cluster 2:2), but also to the emergence of switching regimes (clustered synchronization regimes 3:1 and 2:1:1) characterized by metastability and periodic switching of synchronous states.**

$\sin(\varphi_k - \varphi_j)$ , representing the simplest oscillator interaction. However, accounting for additional physical factors like coupling delays requires generalizing the classical model. The Kuramoto-Sakaguchi model<sup>16</sup> partly fulfills this requirement. Adding a parameter of phase shift  $\alpha$  ( $\sin(\varphi_k - \varphi_j - \alpha)$ ) enables modeling repulsive coupling and more complex interactions<sup>17</sup>.

While the case of attractive coupling ( $\alpha = 0$ ) has been relatively well studied, the dynamics of systems with repulsive coupling ( $\alpha \neq 0$ ) demonstrates significantly richer and often counterintuitive behavior. The work by Tsimring et al.<sup>18</sup> showed that globally coupled identical oscillators with repulsive coupling evolve into a state with a zero mean field, while for non-identical oscillators, complete synchronization for  $N > 3$  turns out to be impossible. It is important to note that for identical oscillators with strictly sinusoidal coupling, the dynamics is partially integrable (Watanabe-Strogatz theory), which imposes strict limitations – for example, it prohibits the formation of stable cluster states, and their observation in numerical experiments is often a discretization artifact<sup>19</sup>. Genuinely complex dynamics, including multiple attractors and complex synchronization regimes, emerges when the conditions of this integrability are violated. This violation can be achieved through different pathways: for instance, through a transition to excitable dynamics of the elements, where global repulsive coupling generates a multitude of periodic regimes via a transcritical heteroclinic bifurcation<sup>20</sup>, or through the introduction of non-identity and mixed interactions, which leads to phenomena such as solitary states and quasiperiodic partial synchrony<sup>21</sup>.

## I. INTRODUCTION

Studying synchronization regimes in ensembles of interacting oscillators across diverse systems is one of main area in nonlinear dynamics. These systems are encountered in biology<sup>1–3</sup>, physics<sup>4,5</sup>, chemistry<sup>6</sup>, neuroscience<sup>7–9</sup>, and other fields. Despite the wide area of practical applications, most of these systems can be reduced to systems of coupled phase oscillators<sup>10–12</sup>. The primary factors complicating the analysis of phase system behavior are individual element dynamics, coupling strength, and interaction topology – global, local, or nonlocal<sup>13,14</sup>.

An important tool for analyzing the behavior of coupled phase oscillators is the Kuramoto model<sup>15</sup>. The classical model considers sinusoidal coupling proportional to

In this work we analyze dynamics in an ensemble of four nonidentical phase oscillators with repulsive coupling. Frequency heterogeneity and repulsive coupling lead to two types of synchronous regimes: stationary and switching.

<sup>a)</sup>Department of Control Theory, Research and Education Mathematical Center "Mathematics for Future Technologies", Lobachevsky State University of Nizhny Novgorod, 23 Gagarin Avenue, Nizhny Novgorod, 603022, Russia

## II. MODEL

The collective dynamics of an ensemble of coupled phase oscillators is described by the Kuramoto-Sakaguchi system [16]:

$$\dot{\phi}_j = \gamma_j + \frac{d}{N} \sum_{k=1}^N \sin(\phi_k - \phi_j - \alpha), \quad (1)$$

where  $j = 1, \dots, N$ ,  $N$  is the number of oscillators,  $\gamma_j$  are the natural frequencies of the oscillators,  $d \in [0, 30]$  is a parameter determining the coupling strength, and  $\alpha$  characterizes the phase shift in the couplings. The interval  $\alpha \in \left(0, \frac{\pi}{2}\right]$  corresponds to attractive coupling, whereas  $\alpha \in \left(\frac{\pi}{2}, \pi\right]$  corresponds to repulsive coupling.

We examine the system with repulsive coupling ( $\alpha = 1.6$ ),  $N = 4$ , and nonidentical natural frequencies uniformly distributed over the interval  $\gamma_j \in [\gamma - \Delta\gamma, \gamma + \Delta\gamma]$ , where  $\gamma = 3, \Delta\gamma = 0.01$ .

## III. SYNCHRONIZATION

In study the collective behavior of oscillators in the Kuramoto-Sakaguchi system, we will focus on various types of both phase and frequency synchronization.

We will distinguish the in-phase synchronous regime, where

$$|\varphi_k(t) - \varphi_j(t)| < c \quad (2)$$

and the anti-phase synchronous regime, where

$$|\varphi_k(t) - \varphi_j(t) - \pi| < c, \quad (3)$$

where the smallness of the value  $c$  depends on the coupling parameter  $d$ . As  $d$  increases, the value of  $c$  approaches 0.

To identify phase ratios between two oscillators, the quantity  $s_{jk} = \sin \frac{\psi_{jk}}{2}$ , defined as the sine of the half-phase difference, i.e.  $\psi_{jk} = \varphi_j - \varphi_k$ , is computed.

- For  $s_{jk} = 1$  anti-phase synchronization is observed ( $\varphi_j - \varphi_k = \pi$ , i.e., the  $j$ -th oscillator leads the  $k$ -th oscillator by  $\pi$ ). We will use the symbol I to denote the anti-phase synchronization:  $\varphi_k \text{I} \varphi_j$ .
- $s_{jk} = -1$  also corresponds to anti-phase synchronization, however  $\varphi_j - \varphi_k = -\pi$ , i.e.  $k$ -th oscillator leads the  $j$ -th oscillator by  $\pi$ .  $\varphi_j \text{I} \varphi_k$ .
- For  $s_{jk} = 0$  in-phase synchronization of two oscillators is observed.
- If  $s_{jk} = s_{nm}$  over a certain time interval, then the phase differences for the oscillator pairs  $j, k$  and  $n, m$  are equal  $\varphi_j - \varphi_k = \varphi_n - \varphi_m$  and  $(\varphi_j - \varphi_k) - (\varphi_n - \varphi_m) = \text{const}$ .

Two oscillators are in a frequency synchronized regime if their *mean frequencies* are equal,

$$\Omega_j = \langle \omega_j \rangle = \Omega_k = \langle \omega_k \rangle, \quad (4)$$

where  $\omega_j = \dot{\phi}_j$  and  $\omega_k = \dot{\phi}_k$  are the instantaneous frequencies of the  $j$ -th and  $k$ -th oscillators, respectively. The frequencies are defined as

$$\Omega_j = \lim_{T \rightarrow \infty} \frac{\varphi_j(T) - \varphi_j(T_0)}{T - T_0}, \quad (5)$$

where  $T_0$  is the transition time.

In addition to synchronization regimes characterized by the equality of mean frequencies, there exist regimes of temporary synchronization (over a certain time interval) where *instantaneous frequencies* coincide,

$$\omega_j = \omega_k. \quad (6)$$

Computational experiments have shown that these intervals of coinciding instantaneous frequencies can be quite prolonged. Furthermore, only two instantaneous frequencies can coincide at any given time.

In the course of the study, for various values of the parameter  $d$  and randomly selected sets of natural frequencies  $\gamma_j$  and initial conditions  $\varphi_j(t = 0)$  (2000 experiments in total), all possible mean frequency synchronization regimes for  $N = 4$  were found. We will separate the sizes of oscillator groups with identical mean frequency by a colon. Then four regimes that are synchronous in mean frequency are possible.

- 4:0 – corresponds to the case, in which all oscillators rotating with the same frequency ( $\Omega_1 = \Omega_2 = \Omega_3 = \Omega_4 = \Omega^s$ ).
- 3:1 – one oscillator has a frequency that differs from the others. For example,  $\Omega_1 = \Omega_2 = \Omega_4 = \Omega_{124}^s \neq \Omega_3$ . This particular realization occurs due to the closeness of the natural frequencies  $\gamma_1, \gamma_2$ , and  $\gamma_4$ ; for a different choice of individual frequencies, oscillators with other indices can synchronize.
- 2:2 – pairwise synchronization. For example,  $\Omega_1 = \Omega_3 = \Omega_{13}^s \neq \Omega_2 = \Omega_4 = \Omega_{24}^s$ . This situation becomes possible due to the pairwise closeness of the natural frequencies  $\gamma_1$  and  $\gamma_3$ , as well as  $\gamma_2$  and  $\gamma_4$ .
- 2:1:1 – two oscillators are in a synchronized state, while the other two have frequencies that differ from those of the synchronized oscillators and from each other. For example,  $\Omega_2 = \Omega_4 = \Omega_{24}^s \neq \Omega_1 \neq \Omega_3$ . The reason for the formation of such ratios is the closeness of the natural frequencies  $\gamma_2$  and  $\gamma_4$ .

The 4:0 regime represents global synchronization, while the 2:2, 3:1, and 2:1:1 regimes correspond to cluster synchronization. In the case of global frequency synchronization, two distinct regimes exist, differentiated by their phase ratios: a splay state, hereafter denoted as  $(4:0)_1$ , characterized by the phase

ratios  $|\varphi_2 - \varphi_1| \cong |\varphi_3 - \varphi_2| \cong |\varphi_4 - \varphi_3| \cong |\varphi_1 - \varphi_4| \cong c_1$ , where  $c_1 = \pi/2$ ; and an in-phase–anti-phase regime, hereafter denoted as  $(4:0)_2$ , for which, for example,  $|\varphi_1 - \varphi_4| < c_2$ ,  $|\varphi_2 - \varphi_3| < c_2$ ,  $|\varphi_2 - \varphi_1 - \pi| < c_2$ ,  $|\varphi_3 - \varphi_4 - \pi| < c_2$ , where  $c_2 \ll 1$ . In this regime, the first and fourth, as well as the second and third oscillators, are nearly in-phase, while the pair comprising the first and fourth oscillators is in anti-phase with the pair comprising the second and third oscillators.

As demonstrated by numerical simulations, the 3:1 and 2:1:1 regimes occur for weak coupling and vanish as it increases. This is because strong coupling compensates for the spread in natural frequencies, forcing oscillators with the most distant frequencies to lock to the majority.

For different combinations of randomly chosen natural frequency sets  $\gamma_j$ , we obtained the dependencies of the mean frequencies  $\Omega_j$  on the coupling strength  $d$ . The results are shown in Fig. 1.

Figure 1 shows examples of the dependence of the mean frequencies on the coupling parameter  $d$  for fixed random initial conditions and two fixed distributions of the natural frequencies  $\gamma_j$ . In the first case (Fig. 1(a)), the natural frequencies are pairwise close, while in the second case (Fig. 1(b)), they are not. Both cases exhibit bistability: either two different 2:2 synchronous regimes coexist (Fig. 1(a)), or a 2:2 synchronous regime and the  $(4:0)_1$  synchronous regime coexist for case (a), or the  $(4:0)_1$  synchronous regime for case (b). Both cases exhibit a 2:2 synchronous regime that persists as parameter  $d$  increases (see inset in Fig. 1(b)). Under constant initial conditions both in Fig. 1(a) and in Fig. 1(b), the global synchronization regimes 4:0 and the cluster synchronization regime 2:2 alternate with increasing value of  $d$ .

In the case where the phase differences are constant in time  $\varphi_k(t) - \varphi_j(t) = \psi_{jk} = \text{const}$ , all mean frequencies are equal, and the formula for calculating the synchronization frequency can be obtained from Eq. (1). From the equality of phase differences it follows that  $\dot{\varphi}_j = \omega_j = \dot{\varphi}_k = \omega_k = \Omega^s$ ; for all  $j, k$ , where  $\Omega^s$  is the mean synchronization frequency. Substituting these conditions into Eq. (1), summing all equations and separating pairs  $j, k$  and  $k, j$ , we obtain the formula:

$$\Omega^s = \frac{1}{N} \sum_{j=1}^N \gamma_j - \frac{2d \sin \alpha}{N^2} \sum_{j < k}^N \cos \psi_{jk}. \quad (7)$$

Eq. (7) in the case of nonidentical natural frequencies is valid only for the 4:0 regime. This formula also reflects the dependence of the mean frequencies  $\Omega_j = \Omega^s$  on the coupling strength  $d$ , where the term  $-\frac{2 \sin \alpha}{N^2} \sum_{j < k}^N \cos \psi_{jk}$  corresponds to the slope of the straight line, and  $\frac{1}{N} \sum_{j=1}^N \gamma_j$  represents the offset relative to the origin.

A special case of Eq. (7) is the uniform phase distribution (the in-phase–anti-phase synchronization regime or splay state). Then the expression for calculating the mean frequency takes the form:

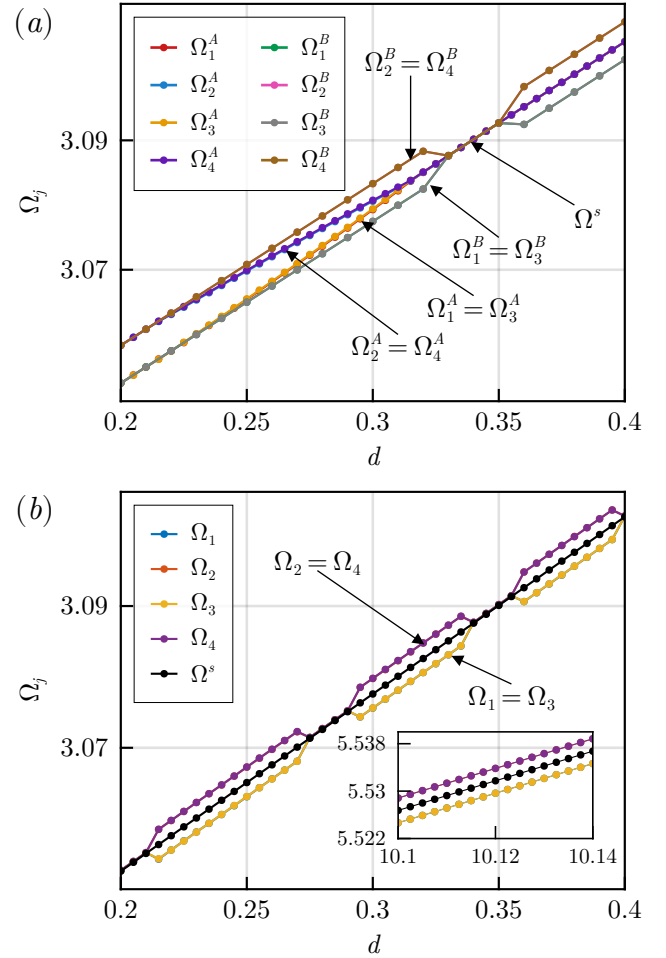


FIG. 1. Dependence of mean frequencies on the coupling strength. Panel (a) corresponds to the case of pairwise practically equal natural frequencies:  $\gamma_1 = 3.00268, \gamma_2 = 3.00821, \gamma_3 = 3.00233, \gamma_4 = 3.00847$ . The superscripts  $A$  and  $B$  denote two experiments with different initial conditions. In experiment  $A$  at a coupling strength of  $d \cong 0.33$ , one of the 2:2 regimes makes a smooth goes (with increasing  $d$ , a gradual reduction of the difference between the mean frequencies within the clusters occurs) to the global synchronization regime  $(4:0)_1$  (see Fig. 2(a)). In experiment  $B$ , for all values of the coupling parameter shown in the figure, a different 2:2 regime exists. Panel (b) corresponds to the case of non-close (compared to the previous case) natural frequencies:  $\gamma_1 = 2.99987, \gamma_2 = 3.00158, \gamma_3 = 3.0053, \gamma_4 = 3.00453$ . In the ensemble, the global synchronization regime  $(4:0)_2$  is realized (Fig. 2(b)). In the inset of Fig. 1(b), the evolution of the mean frequencies at large values of the coupling strength is presented.

$$\Omega^s = \frac{1}{N} \sum_{j=1}^N \gamma_j + \frac{4d \sin \alpha}{N^2} \quad (8)$$

Numerical experiments have confirmed that for the 2:2 regime (an example is shown in Fig. 2(c)), the pairwise synchronization frequencies with increasing coupling strength can be described by the following expressions:

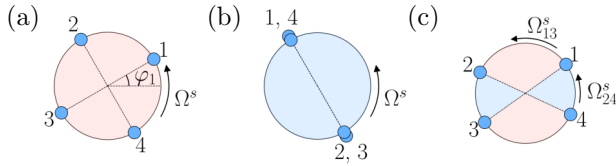


FIG. 2. Phase representation of the 4:0 and 2:2 regimes for large values of the coupling parameter  $d$ . In the case of the 4:0 regimes ((a) – splay state  $(4:0)_1$ , (b) – in-phase–anti-phase synchronization regime  $(4:0)_2$ ), all oscillators rotate with constant frequency  $\Omega^s$ . In the case of the 2:2 regime (c), being in anti-phase, the first and third oscillators rotate with frequency  $\Omega_{13}^s$ , while the second and fourth oscillators, also being in anti-phase, rotate with frequency  $\Omega_{24}^s > \Omega_{13}^s$ .

$$\Omega_{13}^s = \frac{\gamma_1 + \gamma_3}{2} + \frac{4d \sin \alpha}{N^2}, \quad \Omega_{24}^s = \frac{\gamma_2 + \gamma_4}{2} + \frac{4d \sin \alpha}{N^2}. \quad (9)$$

In this regime, one pair of mutually synchronized oscillators (in the example in Fig. 1, the second and the fourth) rotates with a frequency larger than that of the other pair of mutually synchronized oscillators (the first and the third).

According to Eq. (8) and Eq. (9), the synchronization frequencies increase proportionally to the value of the coupling parameter  $d$ : the stronger the coupling, the faster the oscillators rotate.

#### IV. STATIONARY SYNCHRONOUS REGIME

We will call a synchronous regime *stationary* if it exhibits equality of instantaneous frequencies either always (the 4:0 regime) or almost always, except for small time intervals during which the system experiences phase rearrangements (the 2:2 regime). In the case of the 2:2 regime, after a short desynchronization of instantaneous frequencies, the system returns to its original synchronous state.

##### A. 4:0 regime

In the case of the 4:0 frequency synchronization regime, all oscillators rotate with the same constant frequency. Both the means and instantaneous frequencies coincide. Special cases of the 4:0 regime include the splay state  $(4:0)_1$  (Fig. 2(a)) and the in-phase–anti-phase synchronization regime  $(4:0)_2$  (Fig. 2(b)). Fig. 2 illustrates the phase representation of the  $(4:0)_1$ ,  $(4:0)_2$ , for large values of the coupling parameter  $d$ , where the phase ratios characteristic of both regimes are satisfied. Identical coloring of the sectors indicates their equality.

With increasing coupling strength parameter  $d$ , two types of goes to global synchronization regimes were observed: a goes from the 2:2 regime (see subsection IV A) to the 4:0 regime, and a goes from the 3:1 regime (see subsection V A) to the 4:0 regime.

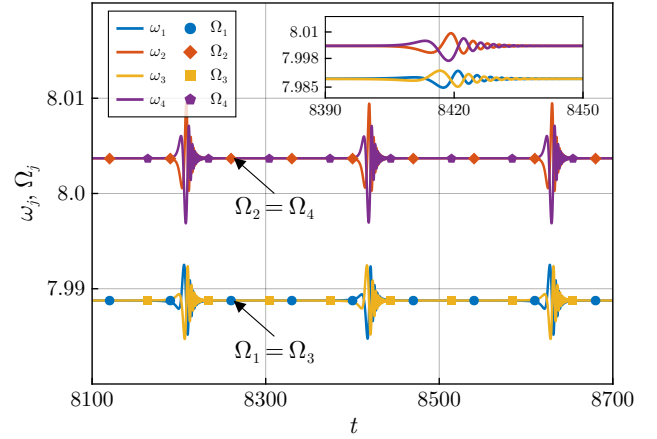


FIG. 3. Evolution of the mean  $\Omega_j$  and instantaneous  $\omega_j$  frequencies for the 2:2 synchronization regime. Parameters: natural frequencies  $\gamma_1 = 2.99086$ ,  $\gamma_2 = 3.00322$ ,  $\gamma_3 = 2.99092$ ,  $\gamma_4 = 3.00842$ , coupling parameter  $d = 20$ . The inset shows the interval of the instantaneous frequencies change.

##### B. 2:2 regime

In the case of the 2:2 regime, the following pairwise equality of mean frequencies occurs:  $\Omega_1 = \Omega_2 \neq \Omega_3 = \Omega_4$ .

In one of the experiments discussed below, with randomly selected natural frequencies  $\gamma_j$ , the following pairwise equality of mean frequencies was observed:  $\Omega_1 = \Omega_3 \neq \Omega_2 = \Omega_4$ .

Figure 3 shows the evolution of the means  $\Omega_j$  and instantaneous  $\omega_j$  frequencies of the 2:2 synchronization regime. In this cluster regime, one pair of oscillators (the second and the fourth) rotates with a mean frequency larger than the rotation frequency of the other pair of oscillators (the first and the third).

In this case, throughout the entire plot, except for intervals corresponding to abrupt changes in instantaneous frequencies (for example, the interval  $\bar{t} \in (8390, 8450)$ , see the inset in Fig. 3), the frequency ratios  $\omega_2 = \omega_4 > \omega_1 = \omega_3$  is observed. For each pair of frequency synchronized oscillators, anti-phase synchronization occurs,  $\varphi_4 - \varphi_2 \cong \pi$ ,  $\varphi_3 - \varphi_1 \cong \pi$  (Fig. 2(c)). During the interval  $\bar{t}$ , short desynchronization (the 1:1:1:1 regime) occurs due to the disruption of phase ratios.

#### V. SWITCHING SYNCHRONOUS REGIME

We will define regime as a *switching* regime if it exhibits metastable dynamics: a relatively long interval of frequency locking between certain oscillators is observed, followed by a short in time desynchronization, after which the system goes to a new synchronous state – frequency locking of other pairs of oscillators – and so on, with the process repeating.

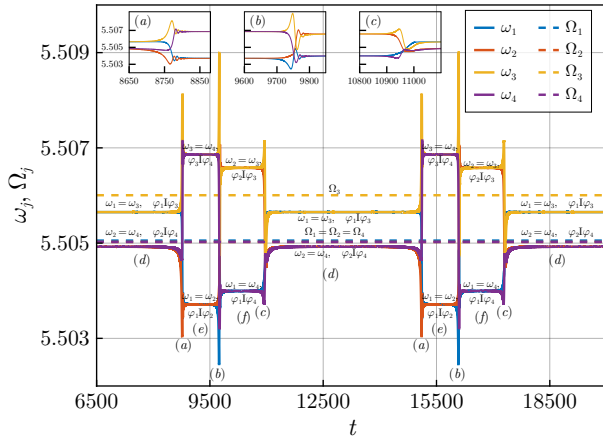


FIG. 4. Evolution of the mean  $\Omega_j$  and instantaneous  $\omega_j$  frequencies for the 3:1 synchronization regime. Parameters: intrinsic frequencies  $\gamma_1 = 3.00385$ ,  $\gamma_2 = 3.00571$ ,  $\gamma_3 = 3.00958$ ,  $\gamma_4 = 3.00627$ ; coupling strength  $d = 10$ . The insets (a), (b) and (c) show magnified views of the corresponding time intervals where the ratios between the instantaneous frequencies change. For a detailed description, see the main text.

### A. 3:1 regime

In the case of 3:1 cluster synchronization, the following coincidence of mean frequencies occurs:  $\Omega_1 = \Omega_2 = \Omega_3 \neq \Omega_4$ .

Fig. 4 shows the evolution of the mean frequencies  $\Omega_j$  and the instantaneous frequencies  $\omega_j = \dot{\varphi}_j$  for a 3:1 synchronization regime. In this particular experiment with the chosen intrinsic frequencies  $\gamma_j$ , the observed regime was characterized by  $\Omega_1 = \Omega_2 = \Omega_4 \neq \Omega_3$ .

Let us consider the time interval  $t \in (7000; 12000)$  and divide it into six subintervals (a)–(f).

In the interval (d) (prior to the first frequency switching), the following conditions:  $\omega_1 = \omega_3$ ,  $\omega_2 = \omega_4$ ,  $\varphi_1 \neq \varphi_3$ ,  $\varphi_2 \neq \varphi_4$ . A similar behavior is exhibited by the frequencies and phases in the interval (e) –  $\omega_3 = \omega_4$ ,  $\omega_1 = \omega_2$ ,  $\varphi_3 \neq \varphi_4$ ,  $\varphi_1 \neq \varphi_2$  and (f) –  $\omega_2 = \omega_3$ ,  $\varphi_2 \neq \varphi_3$ ,  $\omega_1 = \omega_4$ ,  $\varphi_1 \neq \varphi_4$ .

In the intervals (a), (b), and (c), frequency desynchronization occurs, after which the frequencies exhibit distinct behaviors. In the interval (a), the first oscillator initially locks with the fourth, and then with the second. As a result of this frequency switching,  $\omega_3 = \omega_4 > \omega_1 = \omega_2$ . In the interval (b), the fourth and the second oscillators lock with the first and the third, respectively ( $\omega_2 = \omega_3 > \omega_1 = \omega_4$ ). In the interval (c), the first oscillator locks with the third, and the second with the fourth.

Figure 5 shows the evolution of the sine of the half-phase difference for the 3:1 regime.

It should be noted that the plot in Fig. 5 is periodic with a period  $T$ , which coincides with the period of the plot of the mean and instantaneous frequencies in Fig. 4. The value of the period is  $T = t_4 - t_1 = 6365$ . We divide the plot into seven subintervals:  $t_{01} \in (t_0, t_1)$ ,  $t_{12} \in (t_1, t_2)$ ,  $t_{23} \in (t_2, t_3)$ ,  $t_{34} \in (t_3, t_4)$ ,  $t_{45} \in (t_4, t_5)$ ,  $t_{56} \in (t_5, t_6)$ ,  $t_{67} \in (t_6, t_7)$ .

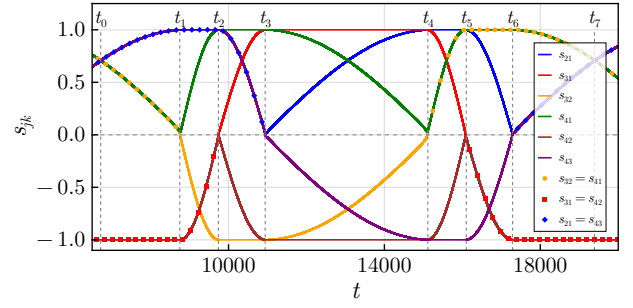


FIG. 5. Evolution of the sine of the half-phase difference  $s_{jk}$ , for the 3:1 regime. Parameters are the same as those in Fig. 4. The lines marked with symbols correspond to the equality of the phase differences for two pairs of oscillators. For a detailed description, see the main text.

In the interval  $t_{01} \in (t_0, t_1)$ , where  $t_0 \cong 6720$ ,  $t_1 \cong 8750$ , the following equalities:  $s_{21} = s_{43}$ ,  $s_{41} = s_{32}$ ,  $s_{31} = s_{42} = -1$ . The last equality means that the oscillators form anti-phase pairs: the third with the first, and the fourth with the second, with  $\varphi_1 > \varphi_3$ ,  $\varphi_2 > \varphi_4$ . Figure 5 shows the plot of the sine of the half-phase difference  $s_{jk}$ , whose indices are listed in reverse lexicographical order. When describing the anti-phase states, we will list first in the pair the oscillator with the larger phase ( $\varphi_1 \neq \varphi_3$ ,  $\varphi_2 \neq \varphi_4$ , in this case). Then, in the case of lexicographical order, the difference is negative, otherwise it is positive. Since, in this time interval, the rotation frequencies of the first and the third oscillators are larger than those of the second and the fourth, one pair overtakes the other; the fourth and the third, and the second and the first oscillators gradually converge, while the fourth and the first, and the third and the second, conversely, diverge. This leads to in-phase–anti-phase synchronization ( $s_{41} = s_{32} = 0$ ) at time  $t_1$  (in Fig. 4, moment  $t_1$  belongs to the interval (a)), after which a frequency switch occurs – a change in the ratio of the instantaneous frequencies.

In the interval  $t_{12} \in (t_1, t_2)$ , where  $t_1 \cong 8750$ ,  $t_2 \cong 9740$ , the third and the fourth oscillators rotate faster than the first and the second ( $\omega_3 = \omega_4 > \omega_1 = \omega_2$ ). Also, for these pairs  $s_{21} = s_{43} = 1$ ,  $s_{31} = s_{42}$ ,  $\varphi_2 \neq \varphi_1$ ,  $\varphi_4 \neq \varphi_3$ . At time  $t_2$  (in Fig. 4, moment  $t_2$  belongs to the interval (b)), in-phase–anti-phase synchronization ( $s_{31} = s_{42} = 0$ ) is achieved, accompanied by a frequency switch.

In the interval  $t_{23} \in (t_2, t_3)$ , where  $t_2 \cong 9740$ ,  $t_3 \cong 10940$ , the second and the third oscillators have larger frequency than the first and the fourth ( $\omega_2 = \omega_3 > \omega_1 = \omega_4$ ) with  $\varphi_4 \neq \varphi_1$ ,  $\varphi_2 \neq \varphi_3$ . As in previous intervals, at time  $t_3$  (in Fig. 4, the moment  $t_3$  belongs to the interval (c)), in-phase–anti-phase synchronization is achieved ( $s_{21} = s_{43} = 0$ ), accompanied by another frequencies switch.

In the interval  $t_{34} \in (t_3, t_4)$ , where  $t_3 \cong 10940$ ,  $t_4 \cong 15115$ , similarly to the interval  $t_{01}$ , the third and the first oscillators have larger frequency than the second and the fourth ( $\omega_1 = \omega_3 > \omega_2 = \omega_4$ ), with the third and the first, as well as the fourth and the second oscillators being in anti-phase. However,  $s_{31} = 1$ ,  $s_{42} = -1$ , or  $\varphi_3 \neq \varphi_1$ ,  $\varphi_2 \neq \varphi_4$ . That is, due to successive frequency switches in pairs of oscillators with

larger and lesser frequencies, at time  $t_3$  the third oscillator becomes anti-phase with the first, and now it is the one leading in phase  $\varphi_3 > \varphi_1$ .

A similar switch is presented in the interval  $t_{45} \in (t_4, t_5)$ , where  $t_4 \cong 15115$ ,  $t_5 \cong 16100$ . Relative to the interval  $t_{12}$ , where  $s_{21} = s_{43} = 1$ , the equality condition splits into two  $s_{21} = 1$ ,  $s_{43} = -1$  ( $\varphi_2 - \varphi_1 = \pi$ ,  $\varphi_3 - \varphi_4 = \pi$ ). Also, in the interval  $t_{45}$ , equality of distances between the fourth and the first, the third and the second oscillators is observed ( $s_{41} = s_{32}$ ).

The evolution of the sine of the phase semi-differences in the interval  $t_{56} \in (t_5, t_6)$ , where  $t_5 \cong 16100$ ,  $t_6 \cong 17290$ , is comparable to the behavior in the interval  $t_{23}$ . However, if in the interval  $t_{23}$  the equality splits into two, then in this case, conversely, a merging occurs. In the interval  $t_{23}$ , the equalities hold:  $s_{41} = 1$ ,  $s_{32} = -1$  ( $\varphi_4 - \varphi_1 = \pi$ ,  $\varphi_2 - \varphi_3 = \pi$ ); in the interval  $t_{56} - s_{41} = s_{32} = 1$  ( $\varphi_4 - \varphi_1 = \varphi_3 - \varphi_2 = \pi$ ), that is, the phase difference between the third and the second oscillators changed from  $-\pi$  to  $\pi$ . Also  $s_{31} = s_{42}$ .

In the interval  $t_{67} \in (t_6, t_7)$ , where  $t_6 \cong 17290$ ,  $t_7 \cong 19390$ , the following equalities hold:  $s_{21} = s_{43}$ ,  $s_{41} = s_{32}$ ,  $s_{31} = s_{42}$ , and the oscillators are in anti-phase  $\varphi_1 \perp \varphi_3$ ,  $\varphi_2 \perp \varphi_4$ . The behavior of the sine of the phase semi-differences is the same as behavior in the interval  $t_{01}$ .

It should be noted that, despite the 3:1 mean frequency synchronization regime, the plot in Fig. 5 (excluding short desynchronization intervals) exhibits an alternation of 2:2 instantaneous synchronization regimes.

## B. 2:1:1 regime

In the case of the 2:1:1 synchronization regime, the following coincidence of mean frequencies is observed:  $\Omega_1 = \Omega_2 \neq \Omega_3 \neq \Omega_4$ .

Let us consider the evolution of the means  $\Omega_j$  and instantaneous  $\omega_j$  frequencies for the 2:1:1 regime (Fig. 6).

The behavior of the oscillators in this case is the same as their behavior in the 3:1 regime. In the interval (e), the following ratios:  $\omega_2 = \omega_3 > \omega_1 = \omega_4$ ,  $\varphi_2 \perp \varphi_3$ ,  $\varphi_1 \perp \varphi_4$ . In the interval (f), the conditions are:  $\omega_3 = \omega_4 > \omega_1 = \omega_2$ ,  $\varphi_2 \perp \varphi_3$ ,  $\varphi_1 \perp \varphi_4$ . The intervals (a), (b), (c), (d) are characterized by the presence of desynchronization; however, in this case, it is not always accompanied by a switch of the frequency synchronization regimes. For example, during the intervals (a) and (c), the relationships  $\omega_1 = \omega_4 > \omega_2 = \omega_3$  and  $\omega_3 = \omega_4 > \omega_1 = \omega_2$  are maintained for each interval, respectively. In contrast, the intervals (b) and (d) exhibit a switch of the frequency synchronization regimes. In the interval (b), the first and the second, and the third and the fourth oscillators are synchronized:  $\omega_1 = \omega_2$ ,  $\omega_3 = \omega_4$ , with  $\omega_3 = \omega_4 > \omega_1 = \omega_2$ . The interval (d) is characterized by a switch of synchronous regimes opposite to that in (b) – the second and the third, and the first and the fourth oscillators are synchronized:  $\omega_2 = \omega_3$ ,  $\omega_1 = \omega_4$ , with  $\omega_2 = \omega_3 > \omega_1 = \omega_4$ .

Figure 7 shows the plot of the evolution of the sines of the phase differences. Similar to the 3:1 regime, the evolution is periodic, with a period  $T = t_3 - t_1 = 4420$ .

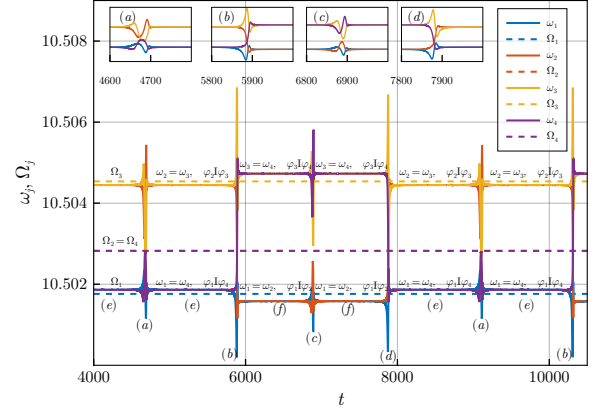


FIG. 6. Evolution of the mean  $\Omega_j$  and instantaneous  $\omega_j$  frequencies for the 2:1:1 regime. Parameters: natural frequencies  $\gamma_1 = 3.00385$ ,  $\gamma_2 = 3.00571$ ,  $\gamma_3 = 3.00958$ ,  $\gamma_4 = 3.00627$ ; coupling strength  $d = 30$ . The insets (a), (b), (c) and (d) show magnified views of the corresponding time intervals where the ratios between the instantaneous frequencies change. For a detailed description, see the main text.

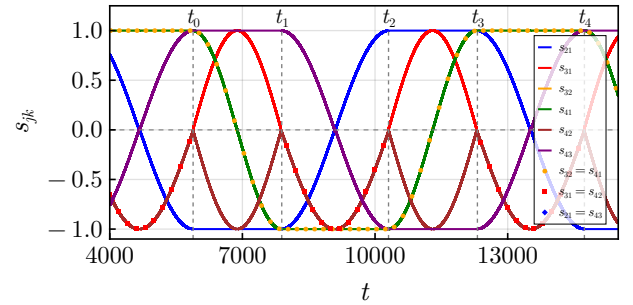


FIG. 7. Evolution of the sine of the phase semi-difference  $s_{jk}$  for the 2:1:1 regime. Parameters are the same as in Fig. 6. Lines marked with markers correspond to the equality of phase differences for two oscillator pairs. For a detailed description, see the main text.

Consider the time interval  $t_{04} \in (t_0, t_4)$  and divide it into four subintervals:  $t_{01} \in (t_0, t_1)$ ,  $t_{12} \in (t_1, t_2)$ ,  $t_{23} \in (t_2, t_3)$ ,  $t_{34} \in (t_3, t_4)$ .

In the interval  $t_{01} \in (t_0, t_1)$ , where  $t_0 \cong 5885$ ,  $t_1 \cong 7890$ , the oscillators rotate in pairs, with the third and the fourth faster than the first and the second ( $\omega_3 = \omega_4 > \omega_1 = \omega_2$ ). The following equalities also hold:  $s_{43} = 1$ ,  $s_{21} = -1$ , i.e.,  $\varphi_4 \perp \varphi_3$ ,  $\varphi_2 \perp \varphi_1$ . Throughout the interval, the same equality  $s_{41} = s_{32}$  is observed between the first and the fourth, and the third and the second oscillators. Here,  $s_{41}$ ,  $s_{32}$  gradually decrease until reaching a splay state, and then further until in-phase–anti-phase synchronization is achieved. The goes of  $s_{jk}$  through zero indicates that one oscillator leads in phase to the other (in this case, the third leads the second and the fourth leads the first). Thus, one pair overtakes the other, exhibiting anti-phase synchronization or, at certain times, a splay state where  $s_{32} = s_{41} = s_{42}$ , or in-phase–anti-phase synchronization (at

time  $t_1$ ), where  $s_{31} = s_{42} = 0$ . The instantaneous frequency switch intervals in Fig. 6 coincide with the phase ratio switch intervals in Fig. 7. Unlike the 3:1 regime, in this case, the frequency synchronization regime switches occur not after every first attainment of in-phase–anti-phase synchronization, but after every second one.

In the interval  $t_{12} \in (t_1, t_2)$ , where  $t_1 \cong 7890, t_2 \cong 10305$ , there also exist two time instances corresponding to the splay state and one instance corresponding to the in-phase–anti-phase synchronization regime. At all other points of the interval, anti-phase synchronization is observed, satisfying the equalities:  $s_{31} = s_{42}, s_{41} = s_{32} = -1$ , which means  $\varphi_1 I \varphi_4, \varphi_2 I \varphi_3$ .

In the interval  $t_{23} \in (t_2, t_3)$ , where  $t_2 \cong 10305, t_3 \cong 12315$ , the evolution of the sine of the phase semi-differences is the same as the behavior in the interval  $t_{01}$ . The second and the first, and the third and the fourth oscillators are in anti-phase; however, compared to the interval  $t_{01}$ , the equalities  $s_{21} = 1, s_{43} = -1$  hold, which means  $\varphi_2 I \varphi_1, \varphi_3 I \varphi_4$ .

In the interval  $t_{34} \in (t_3, t_4)$ , where  $t_3 \cong 12315, t_4 \cong 14735$ , the following equalities:  $s_{31} = s_{42}, s_{41} = s_{32}$ , corresponding to  $\varphi_4 I \varphi_1, \varphi_3 I \varphi_2$ . The second and the first oscillators approach each other, as do the third and the first, and the fourth and the second oscillators, tending towards a splay state and then towards in-phase–anti-phase synchronization ( $\varphi_4 I \varphi_1, \varphi_3 I \varphi_2, \varphi_1 I \varphi_3, \varphi_2 I \varphi_4$ ). After this, the third and the fourth, the third and the first, and the fourth and the second oscillators begin to separate, while the first and the second oscillators approach each other. This leads to the appearance of in-phase–anti-phase synchronization at time  $t_4$  ( $\varphi_4 I \varphi_1, \varphi_3 I \varphi_2, \varphi_4 I \varphi_3, \varphi_1 I \varphi_2$ ).

Similarly to the case of the 3:1 mean frequency synchronization regime, the 2:1:1 regime is characterized by an alternation of instantaneous 2:2 synchronization regimes.

## CONCLUSION

This paper investigates synchronous regimes in an ensemble of four phase oscillators with repulsive coupling and non-identical natural frequencies. All possible frequency synchronization regimes have been identified (4:0 – where all mean frequencies coincide, corresponding to the global synchronization regime; 3:1 – three mean frequencies coincide; 2:2 – pairs of mean frequencies coincide; 2:1:1 – two mean frequencies coincide). These regimes can be classified into two types: stationary and switching. The stationary type includes the 4:0 and 2:2 regimes, characterized by constant synchronization instantaneous frequencies. The 4:0 regime has two types: the splay state (denoted as  $(4:0)_1$ ) and the in-phase–anti-phase synchronization regime (denoted as  $(4:0)_2$ ). In the 2:2 regime, after short in time desynchronization, the system returns to its original synchronous state, preserving groups with equal instantaneous frequencies. In the case of 2:1:1 and 3:1 switching synchronization regimes an alternation of 2:2 instantaneous regimes. According to the derived analytical expressions, synchronization frequencies increase proportion-

ally with coupling strength: stronger coupling leads to faster oscillator rotation.

## ACKNOWLEDGMENTS

The work was supported by the Ministry of Science and Higher Education (project no. 0729-2020-0036 – stationary synchronization) and by the Russian Science Foundation (project no. 22-12-00348 – switching synchronization).

- <sup>1</sup>P. S. Nieto and C. A. Condat, “Translational thresholds in a core circadian clock model,” *Phys. Rev. E* **100**, 022409 (2019).
- <sup>2</sup>J. Merritt and S. Kuehn, “Frequency- and amplitude-dependent microbial population dynamics during cycles of feast and famine,” *Phys. Rev. Lett.* **121**, 098101 (2018).
- <sup>3</sup>A. Prindle and et al., “A sensing array of radically coupled genetic “biopixels,”” *Nature* **481**, 39–44 (2011).
- <sup>4</sup>M. Qian and J.-Z. Wang, “Transitions in two sinusoidally coupled Josephson junction rotators,” *Annals of Physics* **323**, 1956–1962 (2008).
- <sup>5</sup>E. Clerkin, S. O’Brien, and A. Amann, “Multistabilities and symmetry-broken one-color and two-color states in closely coupled single-mode lasers,” *Phys. Rev. E* **89**, 032919 (2014).
- <sup>6</sup>P. S. Smelov, I. S. Proskurkin, and V. K. Vanag, “Controllable switching between stable modes in a small network of pulse-coupled chemical oscillators,” *Phys. Chem. Chem. Phys.* **21**, 3033–3043 (2019).
- <sup>7</sup>E. Izhikevich, *Dynamical Systems in Neuroscience*, Computational neuroscience Dynamical systems in neuroscience (MIT Press, 2007).
- <sup>8</sup>A. Goriely, E. Kuhl, and C. Bick, “Neuronal oscillations on evolving networks: Dynamics, damage, degradation, decline, dementia, and death,” *Phys. Rev. Lett.* **125**, 128102 (2020).
- <sup>9</sup>P. Ashwin, S. Coombes, and R. Nicks, “Mathematical frameworks for oscillatory network dynamics in neuroscience,” *The Journal of Mathematical Neuroscience* **6** (2016).
- <sup>10</sup>A. Pikovsky, M. Rosenblum, and J. Kurths, *Synchronization: a universal concept in nonlinear sciences* (Cambridge University Press, 2001) p. 411.
- <sup>11</sup>A. T. Winfree, “Biological rhythms and the behavior of populations of coupled oscillators,” *Journal of Theoretical Biology* **16**, 15–42 (1967).
- <sup>12</sup>Y. Kuramoto, *Chemical Oscillations, Waves, and Turbulence*, Springer Series in Synergetics, Vol. 19 (Springer Berlin Heidelberg, Berlin, Heidelberg, 1984).
- <sup>13</sup>Y. Kuramoto and D. Battogtokh, “Coexistence of coherence and incoherence in nonlocally coupled phase oscillators,” *Nonlinear Phenom. Complex Syst.* **5**, 380–385 (2002).
- <sup>14</sup>K. Soomin and K. Hiroshi, “Multistability and control in ring networks of phase oscillators with frequency heterogeneity and phase delay,” (2025), arXiv:2502.10681.
- <sup>15</sup>Y. Kuramoto, “Self-entrainment of a population of coupled non-linear oscillators,” in *International Symposium on Mathematical Problems in Theoretical Physics* (Springer, 1975) pp. 420–422.
- <sup>16</sup>H. Sakaguchi and Y. Kuramoto, “A soluble active rotator model showing phase transitions via mutual entertainment,” *Progress of Theoretical Physics* **76**, 576–581 (1986).
- <sup>17</sup>I. León and D. Pazo, “Phase reduction beyond the first order: The case of the mean-field complex ginzburg-landau equation,” *Phys. Rev. E* **100**, 012211 (2019).
- <sup>18</sup>L. S. Tsimring, N. F. Rulkov, M. L. Larsen, and M. Gabbay, “Repulsive synchronization in an array of phase oscillators,” *Phys. Rev. Lett.* **95**, 014101 (2005).
- <sup>19</sup>C. C. Gong, C. Zheng, R. Toenjes, and A. Pikovsky, “Repulsively coupled kuramoto-sakaguchi phase oscillators ensemble subject to common noise,” *Chaos* **29**, 033127 (2019).
- <sup>20</sup>M. A. Zaks and P. Tomov, “Onset of time dependence in ensembles of excitable elements with global repulsive coupling,” *Phys. Rev. E* **93**, 020201 (2016).
- <sup>21</sup>E. Teichmann and M. Rosenblum, “Solitary states and partial synchrony in oscillatory ensembles with attractive and repulsive interactions,” *Chaos* **29**, 093124 (2019).